TGF-β regulates the mechanical properties and composition of bone matrix

Guive Balooch*, Mehdi Balooch*†, Ravi K. Nalla‡, Stephen Schilling§, Ellen H. Filvaroff¶, Grayson W. Marshall*†, Sally J. Marshall*†, Robert O. Ritchie‡, Rik Derynck*‖**††, and Tamara Alliston**††

*Graduate Program in Oral and Craniofacial Sciences, Departments of †Preventive and Restorative Dental Sciences and **Cell and Tissue Biology, and ‖Programs in Cell Biology and Development, University of California, San Francisco, CA 94143; ‡Materials Sciences Division, Lawrence Berkeley National Laboratory, and Department of Materials Science and Engineering, University of California, Berkeley, CA 94720; §Department of Pharmacology and Cancer Biology, Duke University, Durham, NC 27710; and ¶Department of Molecular Oncology, Genentech, South San Francisco, CA 94080

Edited by William D. Nix, Stanford University, Stanford, CA, and approved October 31, 2005 (received for review August 24, 2005)

The characteristic toughness and strength of bone result from the nature of bone matrix, the mineralized extracellular matrix produced by osteoblasts. The mechanical properties and composition of bone matrix, along with bone mass and architecture, are critical determinants of a bone's ability to resist fracture. Several regulators of bone mass and architecture have been identified, but factors that regulate the mechanical properties and composition of bone matrix are largely unknown. We used a combination of high-resolution approaches, including atomic-force microscopy, x-ray tomography, and Raman microspectroscopy, to assess the properties of bone matrix independently of bone mass and architecture. Properties were evaluated in genetically modified mice with differing levels of TGF-β signaling. Bone matrix properties correlated with the level of TGF-β signaling. Smad3+/− mice had increased bone mass and matrix properties, suggesting that the osteopenic Smad3−/− phenotype may be, in part, secondary to systemic effects of Smad3 deletion. Thus, a reduction in TGF-β signaling, through its effector Smad3, enhanced the mechanical properties and mineral concentration of the bone matrix, as well as the bone mass, enabling the bone to better resist fracture. Our results provide evidence that bone matrix properties are controlled by growth factor signaling.

osteoblast | Smad3 | atomic force microscopy

The ability of bones to resist fracture is determined by the bone mass and architecture, and the mechanical properties and composition of the bone matrix (1). Bone architecture is determined by cortical bone thickness, trabecular bone volume, and organization. Several signaling pathways, including estrogen, parathyroid hormone, and TGF-β, have been implicated in the control of bone mass and architecture and its deregulation in metabolic bone diseases such as osteoporosis (2, 3). Much less is known about the mechanical properties and composition of bone matrix, the unique protein- and mineral-rich extracellular material produced by osteoblasts and osteocytes. However, the importance of bone matrix quality is clinically apparent in bone disorders such as osteogenesis imperfecta and osteopetrosis (4, 5). Osteopetrosis patients have increased bone fragility despite elevated bone mass (4). Presumably, bone matrix properties are highly regulated, but the regulators themselves are unknown, partly because of the inaccessibility of methods to define these properties independently of bone mass and architecture. Nevertheless, the regulation of bone matrix properties must be understood to more effectively treat bone disorders.

TGF-β plays stage-dependent roles in osteoblast and osteoclast differentiation. TGF-β inhibits osteoblast differentiation yet stimulates the proliferation of mesenchymal progenitors, thereby expanding the cell population that will differentiate into osteoblasts (6). TGF-β signals through a complex of type I and type II transmembrane serine/threonine kinases (7). Upon ligand binding, the receptor complex phosphorylates the intracellular effector Smad3, which translocates to the nucleus to interact with specific transcription factors to regulate gene expression (7, 8). For example, TGF-β-activated Smad3 binds Runx2 at the runx2 and osteocalcin promoters to repress transcription of genes required for osteoblast differentiation and bone matrix production (9, 10). TGF-β also regulates the expression of osteopontin, osteonectin, type I collagen, and matrix metalloproteinases (11, 12). Because these proteins play roles in bone matrix organization and mineralization (13), the regulation of their expression by TGF-β may affect the material properties of bone matrix.

We used high-resolution biomechanical and imaging techniques to investigate the role of TGF-β signaling in the regulation of the composition and mechanical properties of bone matrix, independently of its effects on bone mass and architecture. These bone matrix properties were defined by using transgenic mice with alterations in TGF-β signaling in their osteoblasts. We found that TGF-β regulates the mechanical properties and mineral concentration of bone matrix, which contributes to its resistance to fracture. Furthermore, reduced TGF-β signaling increased functional parameters of bone quality. These observations identify TGF-β as a key regulator of mechanical properties and composition of the bone matrix and provide evidence that these properties are regulated by cytokines and growth factors.

Materials and Methods

Mice. The phenotypes of Smad3−/−, DNTβRII, D4, and D5 mice are described in refs. 14–17. D4, D5, and DNTβRII mice were bred on a B6D2 background. Smad3+/− and Smad3−/− mice were analyzed in C57Bl6 and 129/C57Bl6 backgrounds, with no detectable background differences. Mutant mice from each line were compared with wild-type littermates. The four wild-type groups were indistinguishable. After euthanasia, femurs, tibiae, and calvarial parietal bones were isolated and cleaned of soft tissue. For histomorphometry and von Kossa staining, tissues were fixed in PBS-buffered formalin (2). X-ray analyses, processing of undecalcified bone sections, von Kossa staining, and histomorphometric analyses were performed as described in refs. 2 and 16. Calvarial osteoblast cultures, RNA isolation, Western analyses, and real-time PCR analysis of Runx2 mRNA were performed as described in refs. 9 and 10. Western analyses were performed by using anti-phospho-Smad3/1 from Cell Signaling Technology (no. 9514) and anti-Smad2/3 from Santa Cruz Biotechnology (FL-425). All studies were repeated on a minimum of three animals. Figures reflect average values or a representative image. Data were analyzed by using one-way ANOVA and post hoc Tukey and LSD multiple comparison tests.

Conflict of interest statement: No conflicts declared.

This paper was submitted directly (Track II) to the PNAS office.

Abbreviations: AFM, atomic-force microscopy; EMM, elastic-modulus mapping; XTM, x-ray tomography.

††To whom correspondence may be addressed. E-mail: tamara.alliston@ucsf.edu or derynck@itsa.ucsf.edu.

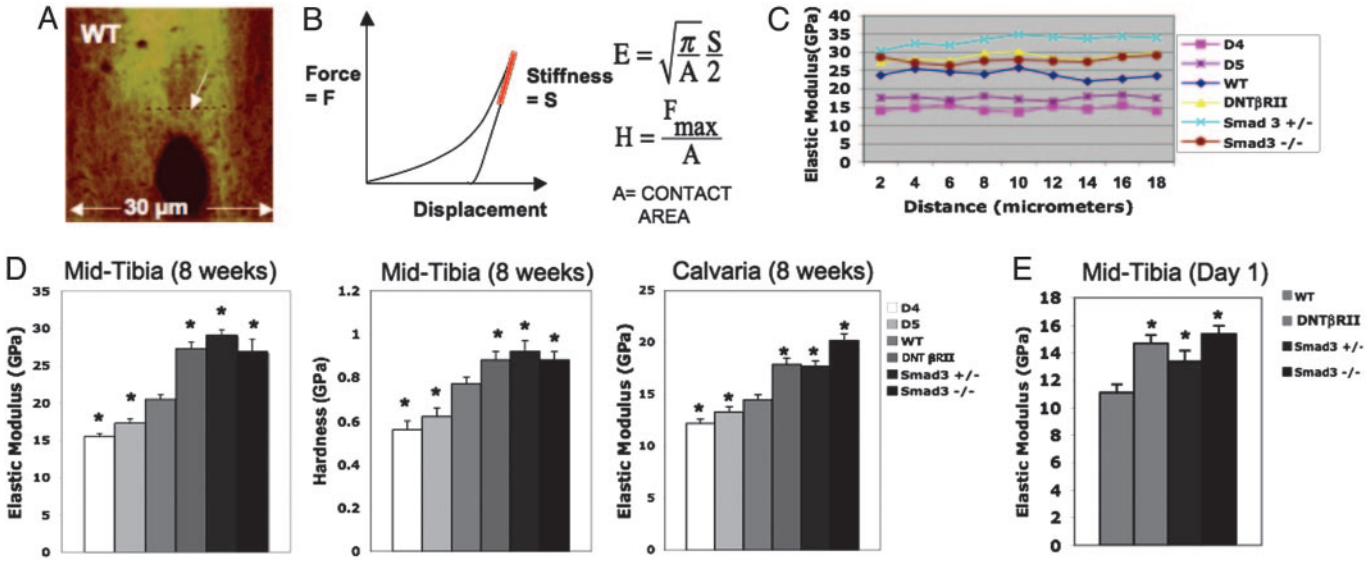

Fig. 1. TGF-β signaling regulates the mechanical properties of bone matrix. (*A*) AFM topography shows a line of nine nanoindentations (arrow) near an osteocyte lacuna. (*B*) Force displacement curves were used to calculate the elastic modulus, *E* (derived from the stiffness, *S*), and hardness, *H*. (*C*) Individual elastic modulus values are for one line of consecutive nanoindentations. Tibia and calvaria from 2-month-old animals with elevated TGF-β signaling (D4 and D5 mice) had decreased elastic modulus and hardness (*D*). Two-month (*D*) and neonatal (*E*) bones with impaired TGF-β signaling (DNTβRII, Smad3+/−, and Smad3−/− mice) had increased elastic modulus and hardness. Error bars show standard deviation. Asterisks indicate a significant difference from wild-type values ($P < 0.001$).

Nanoindentation and Elastic-Modulus Mapping (EMM). Bones embedded in epoxy resin were cross-sectioned and polished as described in ref. 18. An atomic force microscope (AFM) system (Nanoscope III, Digital Instruments) was used to perform nanoindentation testing under dry conditions as described in ref. 19. Nanoindentations with a load range of 300–600 μN produced load-deformation curves, from which the elastic modulus was calculated (Fig. 1*B*). Hardness was calculated based on the contact area, indentation load, and contact stiffness, *S*, defined as the slope of the unloading curve. Sixty serial nanoindentation points, arranged in lines at least 30 μm long with a 2-μm step size, were placed across the mid-tibial cortical bone. Cross-sections of cortical mid-femur, distal tibia, and central parietal bones were also tested. EMM of three or more sections of cortical mid-tibia per animal were performed under the same conditions. Quantitative modulus maps were acquired by using direct-force modulation (18). By using a small sinusoidally modulated force ($\approx$3 μN), EMM measures 256 $\times$ 256 pixels of modulus values with a 15-nm resolution without plastically deforming the material. The measurements and the tip contact radius were calibrated by using a standard quartz sample with known elastic modulus.

Raman Microspectroscopy. An HR-800 Raman spectrophotometer was used, as described in ref. 20, to evaluate organic and inorganic matrix composition of mid-tibial cortical bone that was prepared as for AFM. The HR-800 Raman spectrophotometer uses monochromatic radiation emitted by a HeNe laser (632.8 nm) operating at 20 mW, with a 0.5-μm spot size. Two-dimensional maps were created by using a computer-controlled translation stage to move the specimen in 1-μm increments. Spectra were acquired for the phosphate (PO_4^{3-}) band around 960 cm^{-1} and for the C-H stretching mode (to measure organic content) around 2,900 cm^{-1}.

X-Ray Tomography (XTM). XTM studies were based on the work of Kinney (2, 21), adapted to assess the mineral concentration of bone, as described below. Whole tibias were aligned and embedded in epoxy resin as groups to allow direct comparison of wild-type and mutant bones in the same scan. Imaging with the x-ray source from the Advanced Light Source on beamline (8-3-2) at the Lawrence Berkeley National Laboratory was performed by taking 2D radiographs as the specimens were rotated through 180° in 0.5° increments. The radiographs were reconstructed into 1,000 slices by Fourier-filtered back projection with an 11.7-μm resolution. The attenuation coefficient (mm^{-1}) of each pixel is represented by the false colors and relates directly to bone mineral concentration. Cortical bone thickness was derived from five cortical distance measurements on each of 10 sections per bone.

Macroscopic Mechanical Testing. Fracture toughness testing was conducted on isolated femurs. Samples hydrated in Hanks' balanced salt solution were notched by using a razor blade. Testing was conducted in three-point bending (Fig. 5*A*) with a mechanical testing machine (ELF3200, EnduraTEC), consistent with American Society for Testing of Materials Standard E-399 (22). Samples were loaded to failure in displacement control at 22°C at a cross-head displacement rate of 0.01 mm/s. Fracture surfaces were examined by using scanning electron microscopy. Fracture toughness, K_c, values were calculated by using the stress-intensity solution for a circumferential through-wall flaw in a cylinder (22, 23).

Results

Mouse Models of Increased and Decreased TGF-β Signaling. Because regulators of bone matrix properties have not been identified, and TGF-β regulates bone mass and architecture and the expression of bone matrix proteins (6, 14–17), we examined whether TGF-β regulates the material properties of bone matrix. We used transgenic mice with mutations in TGF-β signaling, including D4, D5, DNTβRII, Smad3+/−, and Smad3−/− mice. D4 and D5 mice express 16- and 2.5-fold increased levels of TGF-β in bone, respectively, under the control of the osteocalcin promoter. D4 bones have more osteoblasts as compared with wild-type mice, reflecting enhanced osteoblast proliferation, but show an age-dependent decrease in volume due to increased bone remodeling (15). The phenotype of D5 bones is similar but less pronounced, consistent with the lower levels of TGF-β expression (15). In contrast, DNTβRII mice, which express a "dominant negative" type II TGF-β receptor in osteoblasts, show decreased TGF-β responsiveness in osteoblasts and increased bone volume (16). Smad3−/− mice,

which are defective in the expression of Smad3 in all tissues, also have a bone phenotype with an osteopenic reduction in bone volume (14, 17). In addition to the direct role of TGF-β/Smad3 signaling in bone metabolism, some aspects of the Smad3$-/-$ bone phenotype may be due to immune, gastrointestinal, or endocrine defects associated with systemic loss of Smad3 expression (24–26). No gross abnormalities have been reported in Smad3$+/-$ mice.

TGF-β Regulates the Mechanical Properties of Bone Matrix. The regulation of bone matrix properties has largely remained uncharacterized, in part because of experimental inaccessibility. To examine the effect of TGF-β on the mechanical properties of bone matrix, independently of macrostructural variation, we used nanoindentation in combination with AFM (19). A representative AFM image of the cortical bone of a wild-type tibia shows a line of nanoindentations near an osteocyte lacuna (Fig. 1*A*). The force-displacement curves (Fig. 1*B*) resulting from nanoindentations were used to calculate the local variations in elastic (Young's) modulus and hardness (19). The elastic modulus is a measure of stiffness, whereas hardness is a measure of strength, specifically resistance to nonelastic deformation under pressure. Bones from 2-month-old mice with altered TGF-β signaling differed in elastic modulus (Fig. 1*C*) and hardness (data not shown) of the bone matrix suggesting that TGF-β regulates these properties.

Similar to a previous study (27), the elastic modulus and hardness of tibial bone matrix of wild-type littermates were ≈20.4 GPa and 0.76 GPa, respectively (Fig. 1*D*). However, bone matrix from DNTβRII mice with reduced TGF-β signaling in osteoblasts had significantly increased elastic modulus and hardness (up to 33%), relative to wild-type littermates (Fig. 1 *D*). In bone where TGF-β signaling was impaired by ablation of Smad3, the elastic modulus and hardness were also significantly increased (42%). This observation suggests that TGF-β acts through Smad3 to regulate the transcription of genes that, directly or indirectly, control bone matrix composition. The elastic modulus was increased, whether osteoclasts retained (DNTβRII) or had impaired (Smad3$+/-$ and Smad3$-/-$) TGF-β responsiveness. Reduced TGF-β responsiveness of osteoblasts is, therefore, sufficient to enhance the bone matrix properties. Because bone mass is reduced in Smad3$-/-$ mice (14, 17) but increased in DNTβRII mice (16), our results also illustrate that the mechanical properties of bone matrix are independent of macrostructural changes in the tissue. Although previous reports had not differentiated Smad3$+/-$ from wild-type bone (14, 17), the elastic modulus and hardness of Smad3$+/-$ bone were as high as the Smad3$-/-$ bone values. In contrast, D4 and D5 mice with elevated TGF-β signaling had lower elastic modulus and hardness, reduced by 24% and 16%, respectively, compared with wild-type littermates. This effect was TGF-β dosage-dependent, because D5 bone, with 2.5-fold elevated TGF-β expression, showed elastic modulus and hardness values in between those for wild-type and D4 bone with 16-fold elevated TGF-β levels (Fig. 1*D*).

Unlike tibiae that are derived through endochondral replacement of cartilaginous precursors, calvaria develop through intramembranous ossification without cartilaginous intermediates. Similar to results for tibial and femoral bone matrix (data not shown), the elastic modulus was higher in calvaria with impaired TGF-β signaling but lower in bone with elevated TGF-β levels (Fig. 1*D*). This finding suggests that the effects of TGF-β on bone matrix mechanical properties are independent of TGF-β's effects on the cartilaginous precursors or the developmental origin of the bone.

To determine whether the TGF-β-regulated differences in bone matrix properties were evident before mature matrix mineralization, we measured the elastic modulus of neonatal (day 1) cortical tibia bone matrix. Although the elastic modulus was considerably lower in neonatal bone than in the 2-month-old bone, reduced TGF-β signaling already resulted in increased elastic modulus in DNTβRII, Smad3$+/-$, and Smad3$-/-$ bone matrix (Fig. 1*E*).

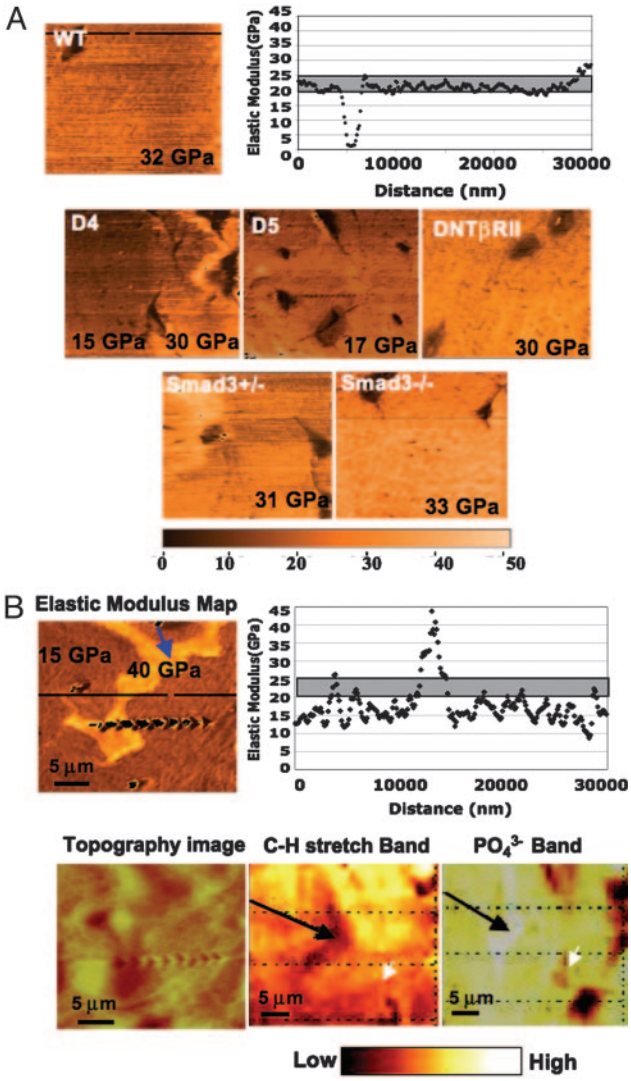

Fig. 2. Mapping of the mechanical properties and composition of bone matrix reveals local variation in D4 bone matrix. (*A*) EMM of mid-tibial cortical bone shows the elastic modulus in a color gradient for the 30-μm^2 area. A graph shows the values corresponding to the black line in the map. Values drop at the site of an osteocyte lacuna. Average values are indicated. (*B*) Only D4 matrix exhibited heterogeneity of elastic modulus (blue arrow) that did not correspond to topography. ''Placemarker'' indents allowed assessment of the same region using Raman microspectroscopy. Modulus variability correlated with heterogeneity of the collagen (C-H stretch band) or hydroxyapatite (PO_4^{3-} band) composition. Lighter colors represent higher Raman peaks. Areas with high mineral and low collagen content (black arrow) had increased elastic modulus, whereas elastic modulus was reduced in areas with low mineral and normal collagen content (white arrow).

These data suggest that the mechanical quality of bone matrix is regulated by the developmental level of TGF-β signaling.

Together, these data indicate a direct relationship between the regulation of gene expression by TGF-β and the mechanical properties of bone matrix of endochondral or intramembranous origin. Increased TGF-β causes deposition of a bone matrix with decreased elastic modulus and hardness, whereas reduced TGF-β signaling causes production of a bone matrix with increased elastic modulus and hardness. Despite differences in bone mass, the similarly increased elastic moduli in Smad3$-/-$ and DNTβRII bone show that TGF-β regulates the mechanical properties of bone matrix independently of bone mass and architecture.

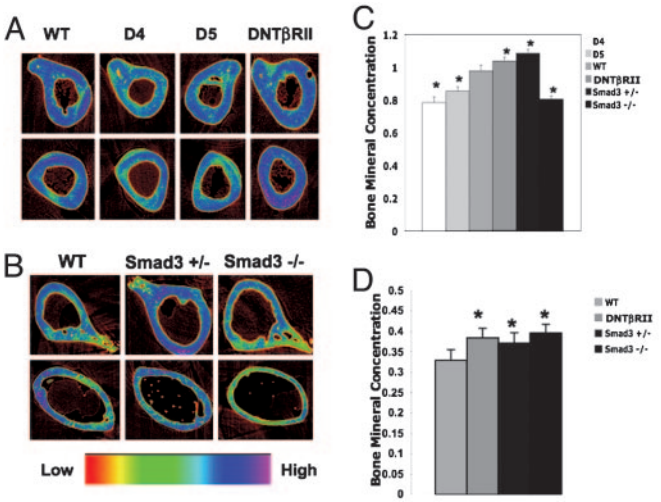

Fig. 3. Effect of TGF-β on bone mineral concentration. Color scales indicate the bone matrix mineral concentration in representative XTM cross-sections through 2-month-old tibia (*A* and *B*). Quantitative analysis of XTM data from 2-month-old (*C*) and neonatal (*D*) bones showed regulation of mineral concentration by TGF-β (*, $P < 0.05$).

Bone Matrix Heterogeneity in Mice with Increased TGF-β Levels. More detailed measurements of mechanical properties were obtained by EMM (18), using much lower force nanoindentations than in previous analyses (Fig. 1). In EMM, elastic modulus is measured without plastic deformation of the bone matrix, thereby enabling high-resolution mapping of a "landscape." This mapping showed no local differences in elastic modulus around lacunae or other physical features. The results are presented in Fig. 2*A* in a linear color scale, with darker areas corresponding to lower elastic modulus values. In addition, each line of modulus data points can be graphically displayed. Consistent with Fig. 1, EMM showed that impaired TGF-β signaling resulted in higher elastic modulus values, whereas elevated TGF-β signaling reduced elastic modulus values, compared with wild-type bone matrix (Fig. 2*A*).

EMM also revealed considerable heterogeneity in the local elastic modulus of D4 bone matrix that was not observed in wild-type mice or in any other mouse lines tested (Fig. 2 *A* and *B*). Although 90% of the D4 bone had a reduced elastic modulus, small patches had a modulus that was higher than in wild-type bone. These high local values did not correlate with the location of osteocyte lacunae. To examine whether they correlated with matrix composition, we used high-resolution (500 nm) Raman microspectroscopy, which maps the mineral (hydroxyapatite) and organic content of bone matrix by measuring peak intensities for PO_4^{3-} at 960 cm^{-1} and C-H stretch at 2,900 cm^{-1} (20). This mapping of the composition revealed considerable local heterogeneity in mineral/organic content in the D4 bone matrix. Certain areas had very high mineral and low collagen content, whereas others had low mineral and normal collagen content. Regions with the highest mineral content had dramatically elevated local elastic modulus values close to 40 GPa. Although the cause remains unknown, this heterogeneity may contribute to the reported tissue-level variability in mineralization (15).

TGF-β Signaling Regulates Bone Mineral Concentration. We also studied the ability of TGF-β to define the relative mineral concentration in bone matrix using synchrotron x-ray computed tomography (XTM) (21). Unlike microCT, XTM uses a monochromatic high-energy x-ray source, and the level of photon absorption correlates directly with the mineral concentration. Elevated TGF-β signaling (D4 and D5) resulted in decreased mineral concentration throughout the tibia compared with wild-type bone from 2-month-old mice (Fig. 3 *A* and *C*). Conversely, reduced TGF-β signaling in DNTβRII or Smad3+/− mice led to increased mineral concentration (Fig. 3 *A–C*), indicating a correlation of the concentration of mineral deposited in the bone matrix with TGF-β signaling. Smad3−/− bone deviated from this relationship, exhibiting reduced mineral concentration compared with wild type (Fig. 3*C*).

Table 1. Summary of TGF-β action on bone quality

Mouse Line	D4	D5	WT	DNTβRII	Smad3+/-	Smad3-/- 1 day	Smad3-/- 8 weeks
TGF-β Signaling	↑	↑	⟺	↓	↓	↓	↓
Elastic Modulus	↓	↓	⟺	↑	↑	↑	↑
Mineral Concentration	↓	↓	⟺	↑	↑	↑	↓
Fracture Toughness	↓	↓	⟺	↑	↑	NS	↓
Bone Mass	↓[14]	↓[14]	⟺	↑[15]	↑	NS	↓[16,17]

NS= not studied, [14-17]See References

Our results correlated TGF-β signaling with hardness, elastic modulus, and mineral concentration of the bone matrix. Increased TGF-β signaling led to diminished mineral concentration and inferior mechanical properties, whereas decreased TGF-β signaling enhanced these properties (Figs. 1 and 3 and Table 1). However, Smad3−/− bones showed reduced mineral concentration, even though DNTβRII and Smad3+/− bones had elevated mineral concentration (Fig. 3*C*). The reported Smad3−/− bone phenotype (14, 17), with its decreased cortical bone thickness and trabecular bone volume, also deviated from what was expected based on the D4, D5, and DNTβ RII bone phenotypes (15, 16). We hypothesized that this discrepancy was a progressive secondary effect on bone resulting from systemic loss of Smad3. Smad3−/− mice exhibit immune, endocrine, and gastrointestinal defects (24–26), any of which might affect bone metabolism. To test this hypothesis, XTM was used to evaluate the mineral concentration of 1-day-old bones when the systemic effects of Smad3 deficiency should as yet be minimal. Before birth, the pup acquires nutrients from the maternal–fetal circulation, bypassing the gastrointestinal system, while the neonatal immune and reproductive systems are immature. As shown in Fig. 3*D*, the mineral concentration in neonatal bone was much lower than in mature bone (Fig. 3*C*). Importantly, neonatal Smad3−/− bone, unlike 2-month-old Smad3−/− bone, had increased mineral concentration relative to wild-type littermates (Fig. 3*D*). The increased mineral concentration (Fig. 3*D*) and elastic modulus (Fig. 1*E*) of neonatal Smad3−/− bone was similar to neonatal DNTβRII bone, in which TGF-β receptor signaling is reduced only in osteoblasts. This finding supports that some properties of the contradictory 2-month-old Smad3−/− bone phenotype are secondary to systemic effects of loss of Smad3. Therefore, before complicating systemic effects on the bone matrix, reduced TGF-β signaling in osteoblasts consistently resulted in increased bone matrix mechanical properties and mineral concentration.

Characterization of the Smad3+/− Bone Phenotype. In the description of the Smad3−/− bone phenotype (14, 17), the Smad3+/− phenotype was presented as similar to wild-type bone. However, our data indicate that Smad3+/− bone matrix differs from wild-type or Smad3−/− bone matrix. We therefore evaluated the mass and architecture of Smad3+/− bones. Consistent with previous reports (14, 17), Smad3−/− femurs had reduced bone mass relative to wild-type femurs when radiographically or histologically assessed (Fig. 4 *A–D*). Surprisingly, Smad3+/− femurs had increased radiodensity relative to wild-type bones (Fig. 4*A*), reflecting increased mineral concentration (Fig. 3*B*) and bone mass (Fig. 4 *B–D*). Thus, Smad3+/− mice possess increased bone mass, whereas Smad3−/− mice have reduced bone mass. Smad3+/−

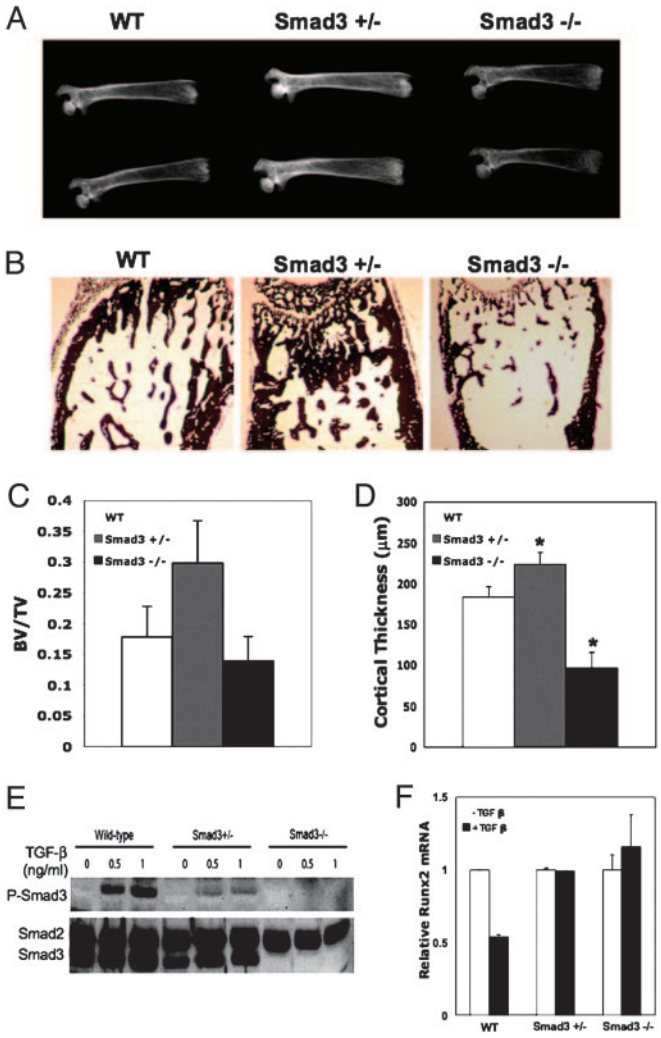

Fig. 4. Increased bone mass in Smad3+/− mice with reduced osteoblast TGF-β responsiveness. X-ray analysis of femurs (*A*) and histomorphometry of von Kossa stained tibiae (*B*) revealed increased radiodensity, trabecular bone volume, and cortical bone thickness in Smad3+/− bone, relative to wild-type and Smad3−/− bone. (*C*) Relative bone volume over total volume, as determined by histomorphometry analysis. (*D*) Differences in cortical bone thickness, as determined by XTM ($P < 0.001$). (*E*) Western analysis shows Smad2 and Smad3 expression and phospho-Smad3 (P-Smad3) in calvarial osteoblast cultures. Cells were treated with TGF-β after 6 h of serum starvation. (*F*) Real-time PCR analysis of Runx2 mRNA expression in calvarial osteoblasts in the absence or presence of 1 ng/ml TGF-β. Values are normalized to RPL19 expression and are shown relative to untreated cells of the same genotype.

bones were most similar, in each parameter assessed, to DNTβRII bones, despite the different approaches used to reduce TGF-β/Smad responsiveness. The similarly increased bone mass, mineral concentration, and mechanical properties in DNTβRII and Smad3+/− bones stand in contrast to the phenotypes of D4 and D5 bones with increased TGF-β signaling (Table 1). The Smad3−/− bone phenotype likely combines bone-specific, i.e., increased osteoblast apoptosis (14), and progressive secondary effects of systemic Smad3 absence on the bone metabolism and health of the mice as mentioned above (24–26).

To further characterize the reduced TGF-β signaling in Smad3+/− versus wild-type bones, we used primary calvarial osteoblasts, cultured from wild-type, Smad3+/−, or Smad3−/− bones. The expression of Smad3 and its activation in response to TGF-β in Smad3+/− osteoblasts were intermediate between wild-type and Smad3−/− cells (Fig. 4*E*). In Smad3+/− cells, the

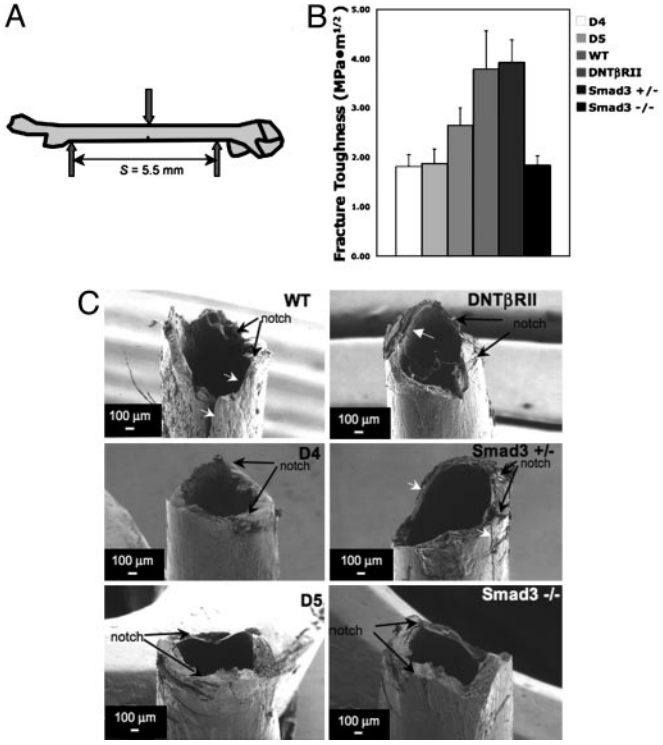

Fig. 5. Fracture toughness of femurs from mice with different levels of TGF-β signaling. A three-point bending test of femurs, where fracture was initiated from a sharpened notch (*A*), was used to measure the fracture toughness of bone, K_c (*B*). Elevated TGF-β signaling (D4 and D5) decreased, whereas reduced TGF-β signaling (DNTβRII and Smad3+/−) increased K_c compared with wild-type bone (*, $P < 0.05$). (*C*) As shown by scanning electron microscopy, fracture-resistant DNTβRII and Smad3+/− bones exhibited extensive crack deflection (white arrows), whereas perpendicular fractures were observed in D4, D5, and Smad3−/− bones. The location of the initiating notch is indicated.

level of Smad3 phosphorylation in response to 1 ng/ml TGF-β was lower than that of wild-type cells treated with 0.5 ng/ml TGF-β (Fig. 4*E*). This reduction in Smad3 activation impacted the ability of TGF-β to inhibit osteoblast differentiation, as assessed by the repression of Runx2 mRNA expression (Fig. 4*F*), alkaline phosphatase activity, and matrix mineralization (data not shown). Therefore, the similarity of the Smad3+/− and DNTβRII bone phenotypes likely results from a comparable reduction in the TGF-β responsiveness of osteoblasts.

Effects of TGF-β on the Macromechanical Properties of Bone. The overall quality of bone is determined by bone mass, architecture, and bone matrix quality; defects in any of these properties predispose bone to fracture. To investigate the role of TGF-β signaling in the macromechanical properties of bone, we subjected femurs to a sharply notched three-point bending test (Fig. 5). The notch in the bone initiates fracture in response to imposed bending stresses, leading to crack propagation (22). The resistance to fracture is expressed as the fracture toughness, K_c, indicating the maximum stress intensity before initiating fracture from the notch.

Femurs from D4 and D5 mice showed a 31% or 29% decrease in fracture toughness, respectively, relative to wild-type bones (Fig. 5*B*). Conversely, bones from DNTβRII or Smad3+/− mice with decreased TGF-β responsiveness exhibited a 43% and 49% higher fracture toughness relative to wild-type, which is consistent with the increased energy to failure in DNTβRII bone (16). Two-month-old Smad3−/− bone had a 30% lower resistance to fracture than did wild-type bone (Fig. 5*B*), consistent with its decreased bone mass (Fig. 4) and bone mineral concentration at this time (Fig. 3). Similar results were obtained for work of fracture (data not shown).

Wild-type, DNTβRII, and Smad3+/− bones exhibited extensive crack deflection, and bone fragments always remained attached after catastrophic fracture (Fig. 5*C*). Such crack deflection increases the energy needed for fracture and may improve the toughness. In contrast, D4 and D5 femurs displayed a more perpendicular fracture, little crack deflection, and complete separation of the bone fragments at failure. Smad3−/− bone showed more crack deflection than D4 and D5 bones, but less than wild-type, DNTβRII, and Smad3+/− bones, perhaps because of the increased elastic modulus and hardness of the Smad3−/− bone matrix (Fig. 1). These data identify TGF-β signaling as a regulator of fracture resistance and show that reduced TGF-β signaling in DNTβRII and Smad3+/− mice increases resistance to fracture.

Discussion

The properties of bone matrix and their regulation by growth factors have remained largely uncharacterized. Using mice with different levels of TGF-β signaling in osteoblasts, we show that TGF-β is a determinant of the material properties of the bone matrix (Table 1). These findings extend our understanding of the role of TGF-β as a regulator of bone mass (6, 14–17) and indicate a relationship between regulation of gene expression by TGF-β, through Smad3, and the mechanical properties of the bone matrix. Using a high-resolution approach, we have demonstrated that growth factor sgnaling can regulate the mechanical properties of bone matrix independently of changes in bone mass and architecture. These critical material properties of the bone matrix should be evaluated, in addition to bone mass and architecture, when studying effects of growth factors, hormones, or drugs on bone quality.

The exact means by which TGF-β signaling regulates the properties of bone matrix remains to be characterized. The role of Smad3 as a mediator of TGF-β signaling in bone is apparent from the similarity of the DNTβRII and Smad3+/− phenotypes. TGF-β and Smad3 regulate osteoblast gene expression, in part by repressing the function of Runx2 (9, 10), a key transcription factor in osteoblast differentiation. Using this and other transcription mechanisms, TGF-β/Smad3 regulates the expression of bone matrix proteins such as osteocalcin, osteopontin, and collagen I (9, 11), each of which can affect matrix mineralization (13). For example, osteocalcin limits the hydroxyapatite crystal formation and increases the resistance to bone fracture (13, 28, 29). Thus, the regulation of gene expression in osteoblasts by TGF-β may affect not only the protein composition, but also the material properties of bone matrix.

Although bone matrix properties and their regulators remain largely uncharacterized, natural and experimental mutations in matrix proteins suggest their importance (5, 30). That bone matrix properties are regulated by TGF-β also has significant physiological and clinical implications. Although the role of TGF-β in osteoporosis remains unclear, mutations have been identified in the TGF-β gene in osteoporotic patients with normal bone mass (31). TGF-β has been implicated in other pathologies involving bone, including bone metastatic tumors, osteoarthritis, and bone fracture (6, 32). TGF-β levels are elevated at sites of tumor metastasis or bone fracture (6, 32). Although TGF-β is required to initiate fracture repair, elevated TGF-β levels, as in D4 and D5 bone, may compromise the material properties of repaired bone matrix.

Our evidence suggests that the Smad3−/− bone phenotype (14, 17) is a combined result of bone-specific and secondary effects of systemic Smad3 loss. At birth, before maturity of the gastrointestinal, endocrine, or immune systems, the mineral concentration of Smad3−/− bone is increased to the same extent as for Smad3+/− and DNTβRII bones (Fig. 3*D*). With maturity, mineral concentration, fracture resistance, and bone mass remain elevated in DNTβRII and Smad3+/− bones (16) (Table 1), but these values drop below wild-type levels in Smad3−/− bones. Together, these observations suggest that the DNTβRII and Smad3+/− phenotypes are more informative of the direct role of TGF-β in bone matrix than the Smad3−/− phenotype. The phenotype of 2-month-old Smad3−/− bone highlights the importance of systemic factors in controlling bone metabolism as well as the primary role of Smad3 in the prevention of premature osteocyte apoptosis and growth plate ossification (14, 17). Similarly, the severe wasting and autoimmune phenotypes of TGF-β1−/− mice may contribute to their reduced bone mass and macromechanical properties (33). We conclude that a reduction of TGF-β signaling in bone increases functional parameters of bone quality, including bone mass, elastic modulus and hardness, mineral concentration, and resistance to fracture. These properties stand in contrast to the phenotypes of D4 and D5 bone, which express elevated levels of TGF-β (Table 1).

Finally, our results suggest that reduction of TGF-β signaling should perhaps be considered as a therapeutic target to treat bone disorders. This is particularly interesting because TGF-β inhibitors are in preclinical or clinical trials for treatment of cancer metastases (34). The possible effects of these agents on bone matrix properties should be investigated.

We thank A. P. Tomsia, J. H. Kinney, R. A. Nissenson, W. Yao, N. E. Lane, G. Nomomura, and S. Ho for their contributions. T.A. is an Arthritis Foundation Investigator. This work was supported by National Institutes of Health grants to R.D., R.K.N., R.O.R., G.B., M.B., G.W.M., and S.J.M., and by the National Center for Research Resources. The Advanced Light Source is supported by the Director, Office of Science, Office of Basic Energy Sciences, of the U.S. Department of Energy under Contract DE-AC02-05CH11231.

1. Currey, J. D. (1999) *J. Exp. Biol.* **202,** 2495–2503.
2. Lane, N. E., Yao, W., Kinney, J. H., Modin, G., Balooch, M. & Wronski, T. J. (2003) *J. Bone Miner. Res.* **18,** 2105–2115.
3. Poli, V., Balena, R., Fattori, E., Markatos, A., Yamamoto, M., Tanaka, H., Ciliberto, G., Rodan, G. A. & Costantini, F. (1994) *EMBO J.* **13,** 1189–1196.
4. Jamsa, T., Rho, J. Y., Fan, Z., MacKay, C. A., Marks, S. C., Jr., & Tuukkanen, J. (2002) *J. Biomech.* **35,** 161–165.
5. Misof, K., Landis, W. J., Klaushofer, K. & Fratzl, P. (1997) *J. Clin. Invest.* **100,** 40–45.
6. Alliston, T. N. & Derynck, R. (2000) in *Skeletal Growth Factors*, ed. Canalis, E. (Lippincott Williams & Wilkins, Philadelphia), pp. 233–249.
7. Feng, X. H. & Derynck, R. (2005) *Annu. Rev. Cell Dev. Biol.* **21,** 659–693.
8. ten Dijke, P. & Hill, C. S. (2004) *Trends Biochem. Sci.* **29,** 265–273.
9. Alliston, T., Choy, L., Ducy, P., Karsenty, G. & Derynck, R. (2001) *EMBO J.* **20,** 2254–2272.
10. Kang, J. S., Alliston, T., Delston, R. & Derynck, R. (2005) *EMBO J.* **24,** 2543–2555.
11. Harris, S. E., Bonewald, L. F., Harris, M. A., Sabatini, M., Dallas, S., Feng, J. Q., Ghosh-Choudhury, N., Wozney, J. & Mundy, G. R. (1994) *J. Bone Miner. Res.* **9,** 855–863.
12. Rydziel, S., Varghese, S. & Canalis, E. (1997) *J. Cell. Physiol.* **170,** 145–152.
13. Hunter, G. K., Hauschka, P. V., Poole, A. R., Rosenberg, L. C. & Goldberg, H. A. (1996) *Biochem. J.* **317,** 59–64.
14. Borton, A. J., Frederick, J. P., Datto, M. B., Wang, X. F. & Weinstein, R. S. (2001) *J. Bone Miner. Res.* **16,** 1754–1764.
15. Erlebacher, A. & Derynck, R. (1996) *J. Cell Biol.* **132,** 195–210.
16. Filvaroff, E., Erlebacher, A., Ye, J., Gitelman, S. E., Lotz, J., Heillman, M. & Derynck, R. (1999) *Development (Cambridge, U.K.)* **126,** 4267–4279.
17. Yang, X., Chen, L., Xu, X., Li, C., Huang, C. & Deng, C. X. (2001) *J. Cell Biol.* **153,** 35–46.
18. Balooch, G., Marshall, G. W., Marshall, S. J., Warren, O. L., Asif, S. A. & Balooch, M. (2004) *J. Biomech.* **37,** 1223–1232.
19. Oliver, W. C. & Pharr, G. M. (2004) *J. Mater. Res.* **19,** 3–20.
20. Schulze, K. A., Balooch, M., Balooch, G., Marshall, G. W. & Marshall, S. J. (2004) *J. Biomed. Mater. Res.* **69A,** 286–293.
21. Kinney, J. H., Haupt, D. L., Balooch, M., Ladd, A. J., Ryaby, J. T. & Lane, N. E. (2000) *J. Bone Miner. Res.* **15,** 1981–1991.
22. Anderson, T. (1994) *Fracture Mechanics: Fundamentals and Applications* (CRC Press, Boca Raton, FL), 2nd Ed.
23. Zahoor, A. (1989) in *Ductile Fracture Handbook* (EPRI, Palo Alto, CA), Report No. NP-6301.
24. Ashcroft, G. S., Yang, X., Glick, A. B., Weinstein, M., Letterio, J. L., Mizel, D. E., Anzano, M., Greenwell-Wild, T., Wahl, S. M., Deng, C. & Roberts, A. B. (1999) *Nat. Cell Biol.* **1,** 260–266.
25. Zhu, Y., Richardson, J. A., Parada, L. F. & Graff, J. M. (1998) *Cell* **94,** 703–714.
26. Tomic, D., Miller, K. P., Kenny, H. A., Woodruff, T. K., Hoyer, P. & Flaws, J. A. (2004) *Mol. Endocrinol.* **18,** 2224–2240.
27. Turner, C. H., Rho, J., Takano, Y., Tsui, T. Y. & Pharr, G. M. (1999) *J. Biomech.* **32,** 437–441.
28. Ducy, P., Desbois, C., Boyce, B., Pinero, G., Story, B., Dunstan, C., Smith, E., Bonadio, J., Goldstein, S., Gundberg, C., *et al.* (1996) *Nature* **382,** 448–452.
29. Roy, M. E., Nishimoto, S. K., Rho, J. Y., Bhattacharya, S. K., Lin, J. S. & Pharr, G. M. (2001) *J. Biomed. Mater. Res.* **54,** 547–553.
30. Fong, H., White, S. N., Paine, M. L., Luo, W., Snead, M. L. & Sarikaya, M. (2003) *J. Bone Miner. Res.* **18,** 2052–2059.
31. Langdahl, B. L., Knudsen, J. Y., Jensen, H. K., Gregersen, N. & Eriksen, E. F. (1997) *Bone* **20,** 289–294.
32. Guise, T. A. & Chirgwin, J. M. (2003) *Clin. Orthop. Relat. Res.* **415,** Suppl., S32–S38.
33. Geiser, A. G., Zeng, Q. Q., Sato, M., Hlevering, L. M., Hirano, T. & Turner, C. H. (1998) *Bone* **23,** 87–93.
34. Dumont, N. & Arteaga, C. L. (2003) *Cancer Cell* **3,** 531–536.